Atmospheric
Measurement
Techniques

Stratospheric CH_4 and CO_2 profiles derived from SCIAMACHY solar occultation measurements

Stefan Noël[1], **Klaus Bramstedt**[1], **Michael Hilker**[1], **Patricia Liebing**[1], **Johannes Plieninger**[2], **Max Reuter**[1], **Alexei Rozanov**[1], **Christopher E. Sioris**[3], **Heinrich Bovensmann**[1], **and John P. Burrows**[1]

[1]Institute of Environmental Physics, University of Bremen, FB 1, P.O. Box 330440, 28334 Bremen, Germany
[2]KIT, IMK-ASF, P.O. Box 3640, 76021 Karlsruhe, Germany
[3]Centre for Research in Earth and Space Science, York University, 4700 Keele Street, Toronto, ON, M3J 1P3 Canada

Correspondence to: Stefan Noël (stefan.noel@iup.physik.uni-bremen.de)

Abstract. Stratospheric profiles of methane (CH_4) and carbon dioxide (CO_2) have been derived from solar occultation measurements of the SCanning Imaging Absorption spectroMeter for Atmospheric CHartographY (SCIAMACHY). The retrieval is performed using a method called onion peeling DOAS (ONPD), which combines an onion peeling approach with a weighting function DOAS (differential optical absorption spectroscopy) fit in the spectral region between 1559 and 1671 nm. By use of updated pointing information and optimisation of the data selection as well as of the retrieval approach, the altitude range for reasonable CH_4 could be broadened from 20 to 40 km to about 17 to 45 km. Furthermore, the quality of the derived CO_2 has been assessed such that now the first stratospheric profiles (17–45 km) of CO_2 from SCIAMACHY are available. Comparisons with independent data sets yield an estimated accuracy of the new SCIAMACHY stratospheric profiles of about 5–10 % for CH_4 and 2–3 % for CO_2. The accuracy of the products is currently mainly restricted by the appearance of unexpected vertical oscillations in the derived profiles which need further investigation. Using the improved ONPD retrieval, CH_4 and CO_2 stratospheric data sets covering the whole SCIAMACHY time series (August 2002–April 2012) and the latitudinal range between about 50 and 70° N have been derived. Based on these time series, CH_4 and CO_2 trends have been estimated. CH_4 trends above about 20 km are not significantly different from zero and the trend at 17 km is about 3 ppbv year^{-1}. The derived CO_2 trends show a general decrease with altitude with values of about 1.9 ppmv year^{-1} at 21 km and about 1.3 ppmv year^{-1} at 39 km. These results are in reasonable agreement with total column trends for these gases. This shows that the new SCIAMACHY data sets can provide valuable information about the stratosphere.

1 Introduction

Carbon dioxide (CO_2) and methane (CH_4) are the most important anthropogenic greenhouse gases. Anthropogenic CO_2 and CH_4 are produced in the troposphere and then, due to their long lifetimes, eventually transported upwards into the stratosphere.

Tropospheric concentrations and/or total column averages of CO_2 and CH_4 are available from both ground-based networks like the Total Carbon Column Observing Network (TCCON, Wunch et al., 2011) and satellite measurements (from 2002 to 2012 by the SCanning Imaging Absorption spectroMeter for Atmospheric CHartographY, SCIAMACHY on Envisat, Bovensmann et al., 1999; Gottwald and Bovensmann, 2011, and since 2009 by TANSO onboard GOSAT, Kuze et al., 2009).

However, especially during the last decade, there has been only very little information available on the stratospheric distribution of CO_2 and CH_4. Since the end of the Envisat mission in 2012, the Atmospheric Chemistry Experiment Fourier Transform Spectrometer (ACE-FTS) on SCISAT (Bernath et al., 2005), launched in 2003, is the only instrument providing CH_4 profiles in the stratosphere (De Mazière et al., 2008). On Envisat, the Michelson Interferometer for Passive Atmospheric Sounding (MIPAS, see e.g. Fischer et al., 2008)

also provided measurements from which stratospheric CH_4 profiles can be inferred (see e.g. Payan et al., 2009).

CO_2 profiling from space is in many cases limited. In particular, the assumption of a known CO_2 volume mixing ratio (VMR) is quite commonly used to determine the altitude at which the instrument is pointing. As a consequence, it is difficult (though not impossible) to determine CO_2 VMRs in these cases. For example, ACE-FTS retrievals use CO_2 to determine pressure and temperature profiles, and thus the altitude grid of the measurements, but CO_2 data in the altitude range between 5 and 25 km (Foucher et al., 2009, 2011; Sioris et al., 2014) and in the mesosphere and lower thermosphere (Beagley et al., 2010; Emmert et al., 2012) can still be derived. For this purpose, N_2 continuum-induced absorption instead of CO_2 absorption is utilised at lower stratospheric altitudes, whereas at mesospheric/thermospheric altitudes the geometrical pointing information is used.

SCIAMACHY pointing information is derived completely independently from CO_2. For the solar occultation data we make use of the method developed by Bramstedt et al. (2012), which determines the precise pointing from scans over the solar disk to determine the position of the solar centre which is then compared to the astronomical position. From this we get an individual pointing correction for each solar occultation measurement which does not depend on the attitude information of the satellite. Therefore, CO_2 concentrations and tangent altitudes can be determined independently from each other.

In this study we present stratospheric profiles of CH_4 and CO_2 which have been derived from solar occultation measurements of SCIAMACHY on Envisat. The retrieval is performed using a method called onion peeling DOAS (ONPD) which is based on an onion peeling approach (see e.g. Russell III. and Drayson, 1972) in combination with a weighting function DOAS (differential optical absorption spectroscopy) fit (see e.g. Perner and Platt, 1979; Burrows et al., 1999; Coldewey-Egbers et al., 2005). A first implementation of this method has been used to retrieve water vapour profiles from SCIAMACHY data (Noël et al., 2010). In a later step, the method had been successfully adapted to CH_4 retrievals (Noël et al., 2011). Within this CH_4 retrieval, CO_2 was also fitted as a secondary absorber. However, in this previous study, not much attention was paid to the quality of the derived CO_2 profiles. Another shortcoming of the retrieval described in Noël et al. (2011) (and the related CH_4 data set V3.3.6) was its restriction to the altitude range from 20 to 40 km.

In the context of the ESA Greenhouse Gas Climate Change Initiative (GHG-CCI), the SCIAMACHY CH_4 and CO_2 profile retrieval has been further improved. The data set used in the present manuscript (V4.5.2) is part of the Climate Research Data Package (CRDP) generated in the context of this project and available via the GHG-CCI web site (www.esa-ghg-cci.org).

We describe the data sets used in this study in Sect. 2, followed by a description of the improved ONPD retrieval (inversion algorithm in Sect. 3 and applied a posteriori corrections in Sect. 4). In Sect. 5 we present the new CH_4 and CO_2 data sets, compare them with independent data and – as an example for a possible application – estimate trends from the derived time series.

2   Data sets used in this study

2.1   SCIAMACHY data

The SCIAMACHY instrument on Envisat measured backscattered earthshine and solar and lunar spectra in nadir, limb and occultation geometry between 2002 and 2012. In this study we use SCIAMACHY radiance spectra measured in solar occultation mode taken from the current level 1 data set, i.e. V7.04, consolidation degree W. SCIAMACHY measures from the UV (about 214 nm) to the SWIR (about 2386 nm). Here we use the spectral interval between 1559 and 1671 nm in which mainly CO_2 and CH_4 absorb light.

The SCIAMACHY solar occultation measurements are performed once per orbit in the Northern Hemisphere during local sunset. However, due to the orbital motion of Envisat, SCIAMACHY sees a rising sun. During a solar occultation measurement, regular scans over the solar disk are performed (see Fig. 1). One upward or downward scan takes 2 s. Typically 16 readouts are taken during one scan, looking at different regions of the sun. The observations start when the sun is still below the horizon by scanning a fixed tangent altitude of around 17.2 km. After the centre of the sun is observed at this tangent altitude, the centre of the scan follows the rising sun until about 100 km.

Above 100 km, two different measurement configurations (so-called "states") were used: for state 47 (executed for typically two orbits per day) the measurement ends with pointing to the solar centre, while for state 49 (executed during the other orbits) the scan over the sun is continued until almost 300 km. In contrast to the algorithm of Noël et al. (2011) the analysis described here uses only data below the 100 km tangent altitude and therefore is applicable to both measurement states.

During a scan over the sun the measured signal varies strongly, because only a small horizontal stripe of the sun (with varying area) is seen during one readout. Furthermore, successive scans over the sun overlap in altitude. In order to avoid large fluctuations with altitude caused by too noisy data, we select a subset of SCIAMACHY occultation data to be used in the retrieval. The basic idea for this selection is to preferably use the data with the highest signal in one scan and to avoid large fluctuations with altitude. The following procedure is used to determine the subset of data to be used in the retrieval.
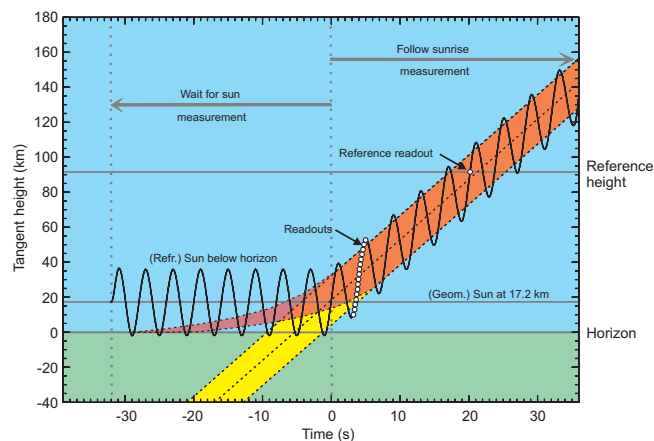
Figure 1. Illustration of the solar scan strategy (modified version of Fig. 2 in Bramstedt et al., 2012). The orange/yellow area indicates the size of the refracted/geometrical sun. The black curve shows the scan as function of time, relative to the time where the geometrical sun reaches 17.2 km (which is the sun-fixed event used in mission planning for this measurement). The white dots indicate (as an example for one upward scan) the position of individual readouts. The corresponding reference readout for an upward scan is also shown.

First, for each readout at a tangent altitude below 60 km the transmittance is computed. For this, we take the measured spectrum and divide it by a reference spectrum measured at around 95 km tangent height. To account for possible systematic differences between upward and downward scans, we use two different reference spectra. An upward reference spectrum is obtained by selecting the spectrum, for one upward scan around this altitude, which has the highest signal outside the absorption (i.e. at the lower edge of the fit window at about 1560 nm). The same is done for a corresponding downward scan to determine the downward reference spectrum.

We then divide the altitude range between 0 and 60 km into 0.5 km bins and select the spectrum with the highest transmittance within each bin. Furthermore, the following additional constraints are applied:

- In order to exclude too noisy data, the transmittance has to be higher than 0.01.

- Without absorption, the transmittance should (at least roughly) increase with altitude. Therefore, a valid transmittance has to be higher than the previous valid transmittance minus 0.02 (when starting from the bottom).

The resulting vertical sampling of data points varies with altitude between about 0.5 and 3 km, with typical average values less than 2 km. This is illustrated in Fig. 2.

2.2 ECMWF data

The ONPD CH₄ and CO₂ retrieval (see Sect. 3) uses pressure and temperature profiles taken from the ECMWF ERA-
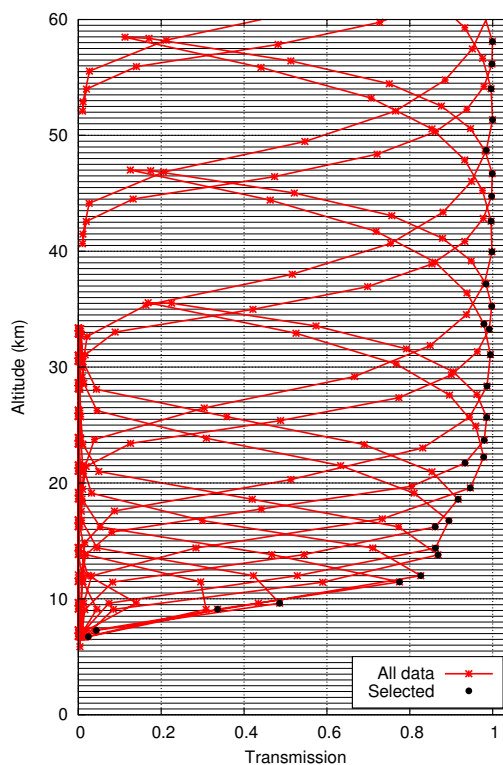

Figure 2. Illustration of selection of data. The transmission at about 1560 nm, i.e. outside the strong absorption, is shown as a function of altitude. Red points show all readouts, connected by lines to illustrate the temporal sequence. Black points show readouts used in the retrieval. The basic idea for the selection is to take the measurements with the highest transmission within one vertical bin of 0.5 km (indicated by horizontal black lines).

Interim data set (Dee et al., 2011) as input. These data are available every 6 h on a $1.5° × 1.5°$ spatial grid. For the retrieval, the model data closest in time and space to an actual measurement are used; no interpolation is performed.

2.3 ACE-FTS CH₄ data

To assess the quality of the derived SCIAMACHY stratospheric CH₄ profiles they will be compared in Sect. 5 with data measured by other sensors. One of these sensors is the Atmospheric Chemistry Experiment Fourier Transform Spectrometer (ACE-FTS) on SCISAT (Bernath et al., 2005) which has provided scientific data since February 2004. In this study, we use the actual ACE-FTS V3.5 CH₄ data product (see Boone et al., 2013, for a description of the retrieval method). The ACE-FTS V3.5 data set is a successor of the V2.2 data, which have been extensively validated (see e.g. De Mazière et al., 2008, for CH₄). De Mazière et al. (2008) state that the overall accuracy of the ACE-FTS V2.2 stratospheric CH₄ product is about 10 % in the upper troposphere and lower stratosphere and about 25 % in the middle and

higher stratosphere. There are no validation results for ACE-FTS V3.5 CH$_4$ data published yet.

For the comparison with SCIAMACHY, we take about 1300 collocated ACE-FTS V3.5 data between 2004 and 2012 based on a maximum spatial distance of 500 km. The maximum temporal distance of these data is usually below 1 h (maximum distance 1.2 h). This is because both ACE-FTS and SCIAMACHY measure in solar occultation geometry and only local sunset data are used, which automatically results in a similar measurement time for collocated data.

2.4   HALOE data

The Halogen Occultation Experiment (HALOE; Russell III. et al., 1993) on the Upper Atmospheric Research Satellite (UARS) provided the longest stratospheric CH$_4$ time series so far (1991–2005). HALOE measured in solar occultation viewing geometry both during sunset and sunrise. In this study, we use HALOE sunset data v19 for the comparison with SCIAMACHY, because SCIAMACHY solar occultation spectra are also measured during sunset. The precision of HALOE CH$_4$ profiles is in the order of 7 %, while the total uncertainty including systematic errors is about 15 % (Park et al., 1996, based on v17 HALOE data).

Because the HALOE time series ends in August 2005, the temporal overlap with SCIAMACHY is only three years. To achieve a suitable number and temporal distribution of collocations, we chose a maximum spatial distance of 800 km, which results in about 300 collocations. We only use HALOE sunset data; therefore the temporal mismatch to SCIAMACHY is also very low here (< 1 h).

2.5   MIPAS data

The SCIAMACHY CH$_4$ data have also been compared with stratospheric CH$_4$ profiles obtained by the Michelson Interferometer for Passive Atmospheric Sounding (MIPAS; Fischer et al., 2008), which is also part of the Envisat atmospheric chemistry payload. MIPAS performed measurements in limb viewing geometry. The MIPAS measurements cover the time interval between 2002 and 2012. Until 2004 MIPAS was operated in the so-called high-resolution (HR) mode, but later on in reduced- resolution (RR) mode, i.e. with lower spectral resolution but higher spatial resolution.

The MIPAS profiles used in this study were derived with the research processor developed at the Institute of Meteorology and Climate Research and at the Instituto de Astrofísica de Andalucía (CSIC) (von Clarmann et al., 2003). Versions are V5H_CH4_20 for the time interval from 2002 to 2004 in combination with V5R_CH4_222 (for January 2005–April 2011) and V5R_CH4_223 (for May 2011–April 2012). Note that the only difference between V5R_CH4_222 and V5R_CH4_223 is the source of ECMWF data used as a priori in the temperature retrieval, which has a negligible impact on the CH$_4$ product. The accuracy of the MIPAS CH$_4$

profiles is expected to be high in the middle stratosphere as no clear bias to other sensors is observed; however, below about 25–30 km MIPAS CH$_4$ seems to have a high bias on the order of 0.2 ppmv (Laeng et al., 2015).

For the selection of collocated data from MIPAS we used the same maximum spatial distance of 800 km as for HALOE, but the maximum temporal distance was chosen to be 9 h, taking into account that MIPAS performed about 72 limb measurements per orbit in HR and 96 in RR at varying local times, whereas there was only one SCIAMACHY solar occultation measurement per orbit at local sunset. Because of the different viewing geometries, it is not possible to restrict the maximum temporal offset to about 1 h (as for ACE-FTS and HALOE), as this would result in no collocations with MIPAS. With the chosen criteria, we usually obtained several MIPAS measurements which match with one SCIAMACHY measurement, from which we selected the closest one (spatially). This results in more than 25 000 collocations between August 2002 and April 2012, which essentially cover all seasons.

2.6   ACE-FTS CO$_2$ data

One of the stratospheric CO$_2$ data sets used in this study is derived from ACE-FTS measurements and based on the algorithm by Sioris et al. (2014). It is a research data product which covers the years 2009 to 2011. Profiles are available for altitudes below 25 km. There are about four data points above 17 km. The data set used here is a combination of V4.3 and V4.4 data; these versions only differ in the choice of pressure and temperature profiles below 15 km, which are not relevant for this study. We use the same collocation criteria as for the ACE-FTS CH$_4$ data, i.e. only sunset data with a maximum distance of 500 km. This results in about 100 collocations.

2.7   CarbonTracker data

To our knowledge there are no measured stratospheric CO$_2$ profiles covering the full spatial and temporal range of the SCIAMACHY solar occultation data. The standard ACE-FTS CO$_2$ product only contains measurement results at mesospheric altitudes (above about 70 km), whereas the CO$_2$ values below are based on a simple equation (see Boone et al., 2005). The stratospheric CO$_2$ data from ACE-FTS used in this study are based on a research product and only cover altitudes below 25 km (see above). In addition to a comparison with these data, the quality of the ONPD CO$_2$ profiles is assessed in Sect. 5 by comparison with data derived from the CarbonTracker model (Peters et al., 2007). Here, we use the latest version of these model data (CT2013), which cover the time interval until the end of 2012.

For each SCIAMACHY measurement the spatially and temporally closest CT2013 profile has been selected, resulting in a collocation for each of the SCIAMACHY profiles.

The CarbonTracker VMR data, which have a quite coarse sampling of about 5 km in the stratosphere, have then been interpolated to the 1 km altitude grid of the SCIAMACHY data.

3 Inversion algorithm

The ONPD algorithm is essentially based on a weighting function DOAS fit (see e.g. Perner and Platt, 1979; Burrows et al., 1999; Coldewey-Egbers et al., 2005) in combination with an onion peeling approach (see e.g. Russell III. and Drayson, 1972).

We divide the atmosphere into N spherical layers. The absorptivity of the whole atmosphere can then be written as the sum of the absorptions of these individual altitude layers. Let $c_{i,k}$ be the atmospheric parameter associated with the absorption features in atmospheric layer i. This could, for example, be the number density of an absorber k. It is then the task of the retrieval to determine the vertical profile of c as a function of height (index i) for each absorber (index k). As typical for an onion peeling approach, the retrieval starts at the top layer and propagates downwards, taking into account the results of the upper layers.

The basic equation of the ONPD method for a tangent altitude j is then given by the following:

$$\ln\left(\frac{I_j}{I_0}\right) = P_j + \ln\left(\frac{I_{j,\text{ref}}}{I_{0,\text{ref}}}\right) + \sum_{k=1}^{M}\sum_{i=1}^{N} w_{ij,k}\, a_{i,k}, \qquad (1)$$

where M is the number of absorbers; I_j is the measured radiance for tangent altitude j; I_0 is the corresponding radiance obtained at the reference altitude, i.e. at an altitude which is high enough that atmospheric absorption can be neglected.

The ratio I_j/I_0 is therefore the measured atmospheric transmittance. $I_{j,\text{ref}}$ and $I_{0,\text{ref}}$ are the corresponding values calculated for a reference scenario (i.e. for a reference set of parameters c_{ref}).

The quantity $w_{ij,k}$ describes – similar to a relative weighting function – the change of the (logarithmic) transmittance when changing the atmospheric parameter (evaluated at $c_{i,k,\text{ref}}$):

$$w_{ij,k} := c_{i,k,\text{ref}} \left.\frac{\partial \ln(I_j/I_0)}{\partial c_{i,k}}\right|_{c_{i,k,\text{ref}}}, \qquad (2)$$

where $w_{ij,k}$ is determined using the radiative transfer model SCIATRAN 3.3 in transmission mode (Rozanov et al., 2014). The solar irradiance spectrum used in this context has been derived from an empirical solar line list provided by G. Toon (NASA Jet Propulsion Laboratory). The SCIATRAN calculations take into account the effects of refraction and the vertical size of the SCIAMACHY field of view (0.045°). A main advantage of the weighting function DOAS method is that it is possible to handle dependencies on pressure and temperature in a similar way to absorbers, i.e. by definition of appropriate weighting functions. The parameter c can therefore be any parameter on which the measured transmittance depends. This may be the number density of an atmospheric constituent as well as pressure or temperature.

The scalar $a_{i,k}$ is defined as the relative change of $c_{i,k}$:

$$a_{i,k} := \frac{\Delta c_{i,k}}{c_{i,k,\text{ref}}} = \frac{c_{i,k} - c_{i,k,\text{ref}}}{c_{i,k,\text{ref}}}. \qquad (3)$$

As typical for DOAS-type retrievals, broadband absorption features (e.g. from aerosols) and uncertainties in the radiometric calibration are handled via a low-order (in the present case second-order) polynomial P_j. Furthermore, uncertainties in the spectral calibration are accounted for by fitting additional spectral shift and squeeze factors.

The retrieval starts at the top of the atmosphere and then propagates downwards. A non-linear least squares fit (Levenberg–Marquardt algorithm) is used to determine from Eq. (1) for each tangent altitude the shift and squeeze parameters, the coefficients of P_j and the corresponding $a_{j,k}$. The noise of the measurement data is not considered in the fit.

Note that – in contrast to the previous retrieval version described by Noël et al. (2011) – the summation over altitude (index i in Eq. 1) now also includes altitudes below the tangent height. With this we account for effects due to refraction and the vertical smearing of the signal by the instrument field of view. Because of refraction, the light path through the atmosphere is no longer a straight line but bent such that atmospheric layers from below the tangent altitude also affect the measured signal. However, because of the onion peeling approach, there is no information about altitudes below the current tangent height j. As an approximation, we therefore assume in the retrieval that $a_{i,k} = a_{j,k}$ for all altitudes $i < j$. This means that we assume that all parameters c below the current altitude j scale the same way as for j. Noting that the contributions from altitudes below the current tangent height are typically small and limited to a few kilometres, this is a reasonable assumption. This means that for each atmospheric parameter only one $a_{j,k}$ needs to be determined in one retrieval step.

From the retrieved $a_{j,k}$ the parameter $c_{j,k}$ (e.g. the number density of the absorber k at altitude j) can then be determined (see Eq. 3):

$$c_{j,k} = (1 + a_{j,k})\, c_{j,k,\text{ref}}. \qquad (4)$$

This type of retrieval may in principle be applied to all kinds of species/spectral regions. The selected fit window and the related absorptions determine the number of absorbers to be considered. In the present case we choose the fit window to be 1559–1671 nm. We consider CH_4 and CO_2 as absorbers, and temperature and pressure as additional parameters. However, only CH_4 and CO_2 number densities are determined in the fit; adequate pressure and temperature profiles are provided as input to the retrieval and kept unchanged to reduce the impact of correlations between

the weighting functions (especially regarding pressure and CO_2). For the current product version (V4.5.2), the radiative transfer database has been calculated assuming the 1976 US Standard Atmosphere with background stratospheric aerosol and an altitude-independent CO_2 VMR of 380 ppmv. In the retrieval, input temperature and pressure profiles are taken from collocated ECMWF ERA-Interim data (Dee et al., 2011). Weighting functions are then used to correct differences to the settings in the radiative transfer calculations.

The ONPD retrieval has several advantages. First of all, it is a simple method which may be applied to various spectral regions. Furthermore, no individual radiative transfer model calculations are required during the retrieval, because a pre-calculated database can be used for the weighting functions and the reference transmittances. This database has been calculated on a high spectral sampling grid, which is then interpolated in the retrieval to the wavelength grid of the measured spectra. This makes the method numerically very fast.

In the present case, the retrieval uses an altitude grid which reaches from 0 to 50 km in 1 km steps. The retrieval is then performed for all altitudes above 10 km (starting at 50 km), but due to tropospheric effects, e.g. strong refraction at lower altitudes and low signal-to-noise at higher stratospheric altitudes, useful results for CH_4 and CO_2 are only achieved between 17 and 45 km.

Because the onion peeling method uses a pre-calculated radiative transfer database, it is necessary to interpolate the logarithms of the SCIAMACHY measured transmission spectra to the 1 km retrieval grid. To increase the stability of the interpolation towards e.g. noise effects, we normalised each spectrum before the interpolation to its average value. This is possible, because the ONPD retrieval is not sensitive to absolute radiometric calibration (which is handled via the polynomial). The vertical interpolation is then done using Akima splines.

An example for a fit at 25 km and the corresponding residual is shown in Fig. 3. The two absorption features between 1560 and 1620 nm are attributed to CO_2. The absorption above 1620 nm is mainly due to CH_4, with some underlying contributions from CO_2. As can be seen from this plot, the amplitude and variability of the residuals are higher above about 1590 nm and largest around 1645 nm. This is due to a change in the SCIAMACHY detector material, which results in higher measurement noise at the longer wavelengths. This already implies that the precision of the derived CO_2 is higher than for CH_4.

After the retrieval, we apply some additional corrections. These are described in Sect. 4. Finally, we derive VMRs from the retrieved number densities using the same pressure and temperature profiles which we assumed in the retrieval, i.e. the corresponding ECMWF data for this measurement.
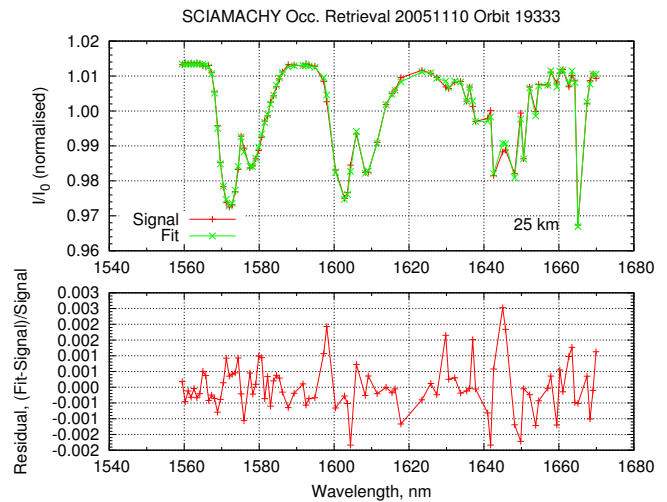

Figure 3. Example of a spectral fit. Top: normalised measured spectrum (red) and fitted spectrum (green) at 25 km tangent altitude. Bottom: resulting residual, i.e. relative difference between measurement and fit.

4 Corrections

4.1 Error correction

In the onion peeling approach only the density scaling factors for the actual tangent height j are fitted, i.e. the $a_{j,k}$ for each absorber k (see Eq. (1) and the description given in the previous section). For a fit at tangent height j it is assumed that all $a_{i,k}$ from below ($i < j$) are identical to $a_{j,k}$ and all $a_{i,k}$ from altitudes higher than j are known from previous fits. The error for $a_{j,k}$ is the fit error, which is derived from the covariance matrix of the fit parameters obtained in the fit and scaled with the root mean square of the fit residual. This accounts for the unweighted fit.

Calculating the error in this way implies that all $a_{i,k}$ for $i > j$ are assumed to have no error (although the error is in fact determined in previous fits). The error for $a_{j,k}$ derived from the fit is therefore overestimated because it also includes the errors from the upper altitudes.

To account for this effect, the retrieved errors have been multiplied by a factor of 0.66. This value has been derived by application of standard error propagation to about 10 000 retrievals on measurement data. In this context, the error obtained from the retrieval at one altitude has been propagated downwards in an onion peeling way. From this it turns out that the required error correction factor is quite independent from the observed scene and almost constant over altitude. The factor is also the same for CH_4 and CO_2, thus indicating that the correlation of the fit parameters is about constant with altitude and thus essentially determined by geometry.

Note that, although the average error correction factor is constant, the exact determination of the individual errors introduces, especially at higher altitudes (where measurement

noise is larger), additional oscillations in the retrieved errors, which is a typical problem of onion peeling methods (see also the following section). This is why we prefer to use an average error correction here.

4.2 Vertical smoothing

Although the retrieval is performed on a 1 km altitude grid, the vertical resolution of a single SCIAMACHY measurement is limited by the vertical size of the field of view (0.045°), which corresponds to about 2.6 km at the tangent point. The size of the field of view has been considered in the radiative transfer calculations, which effectively results in a vertical smoothing of the reference spectra profiles and the weighting functions profiles.

In contrast to many optimal estimation type retrievals, the ONPD method does not include a regularisation. This especially means that the smoothness of the resulting profiles is not constrained in the retrieval, such that artificial oscillations over altitude are not suppressed. This is a general problem of the onion peeling approach: if, for example, a too high value is retrieved at one altitude, this is compensated by a too low value at the next altitude. In the present case we account for this lack of regularisation by vertically smoothing the retrieved profiles (scaling factors) using a boxcar of width 4.3 km. This width has been chosen because it corresponds to the approximate vertical range covered by the scan over the sun during one integration time. However, this is in fact an arbitrary choice resulting from a trade-off between vertical resolution and amplitudes of oscillations in the profiles.

Since boxcar smoothing is similar to averaging, the error of the retrieved scaling factors is reduced after smoothing. Assuming that the error is random and the underlying data are uncorrelated, this would result in a factor of $\sqrt{4.3}$. This is in fact a conservative estimate since – as explained above – adjacent altitudes are typically anti-correlated. On the other hand, smoothing does not affect systematic errors contained in the spectra, but since the systematic errors are unknown, there is no way to quantify this effect. On a best effort basis, the error of the final data product is therefore estimated to be reduced by $\sqrt{4.3}$ due to smoothing. This error reduction factor is considered to be of similar quality as the broadband error correction described in the previous section, which assumes a constant scaling factor for all altitudes.

As can be seen from Fig. 4, the smoothing is quite efficient although the smoothing procedure cannot fully remove oscillations of the correction factor (and therefore derived densities) with altitude. This issue will be addressed further below.

4.3 Saturation correction

Atmospheric absorbers like CH_4, CO_2, O_2 or water vapour have strongly varying absorption lines which are not resolved by the SCIAMACHY instrument because of its too low
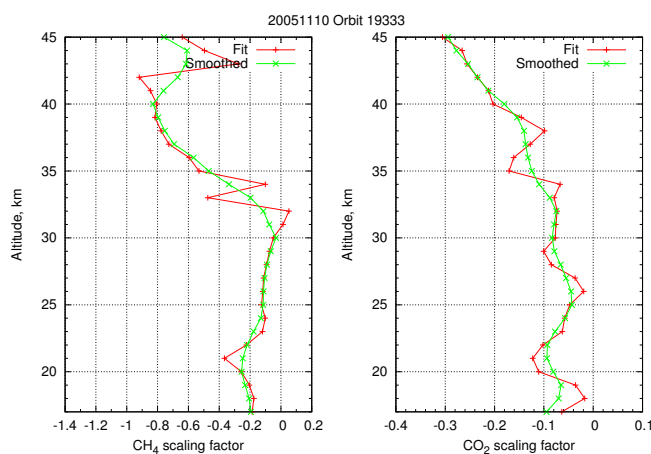

Figure 4. Example for derived profile scaling factors a from SCIA-MACHY solar occultation for CH_4 (left) and CO_2 (right). Red shows the original fit result, green shows vertically smoothed data.

spectral resolution. The signal measured by SCIAMACHY is therefore comprised of a convolution of saturated and non-saturated lines. As a consequence, the relationship between absorber amount and absorption depth becomes non-linear, which is usually referred to as saturation effect. Thus, the weighting function depends on the chosen linearisation point, i.e. the reference concentration assumed in the radiative transfer calculations.

We account for this effect by application of a saturation correction function. This function is determined from retrievals on a set of simulated spectra, which are based on scaled profiles of the absorber to be corrected. The ratio of the true to the retrieved number density then gives the saturation correction. We store the (simulated) true and retrieved densities in a look-up table and then derived the actual density at a certain altitude by interpolation to the retrieved number density.

The determined correction functions are shown in Fig. 5a for CH_4 and Fig. 5d for CO_2.

The weighting functions – and through this, the retrieved CH_4 and CO_2 density – also depend slightly on the actual pressure and temperature, which might differ from the assumptions in the radiative transfer calculations. Note that although the CO_2 VMRs are rather constant, the CO_2 number densities vary with temperature and pressure. We therefore determine additional corrections for CH_4 and CO_2 depending on the actual pressure and temperature. These corrections are multiplicative factors (shown in Fig. 5b, c, e and f). They are determined in a similar way as the saturation correction (i.e. we apply the retrieval to a set of simulated data, but now we keep CH_4 and CO_2 fixed and vary (scale) pressure or temperature profiles).

These correction factors are also stored in a look-up table from which actual factors are obtained by interpolation to the retrieved quantity for each altitude. Since pressure
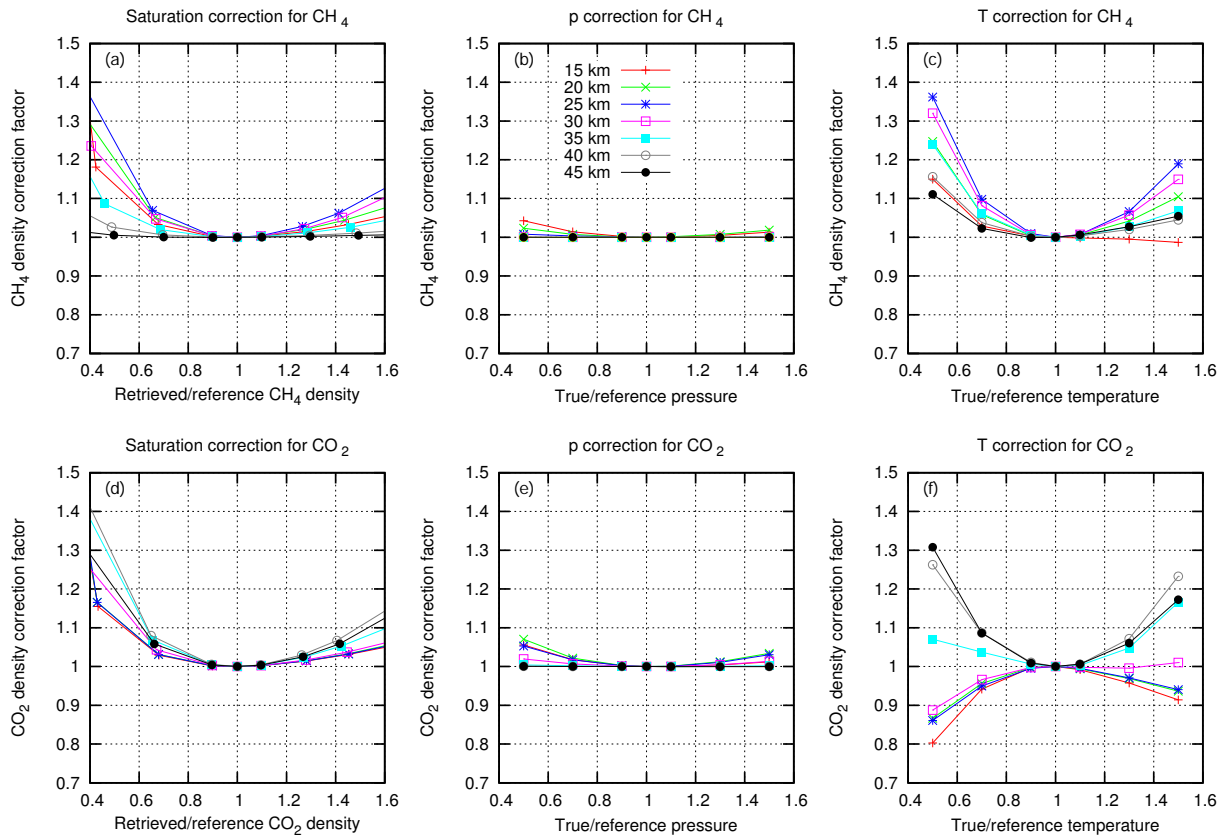
Figure 5. (a) Saturation correction factors for CH$_4$. **(b)** Pressure correction factors for CH$_4$. **(c)** Temperature correction factors for CH$_4$. **(d)** Saturation correction factors for CO$_2$. **(e)** Pressure correction factors for CO$_2$. **(f)** Temperature correction factors for CO$_2$.

and temperature are not retrieved in the fit but taken from ECMWF data, the applied pressure and temperature corrections account for the difference between the ECMWF pressure/temperature used as input profiles in the retrieval and the pressure/temperature assumed in the radiative transfer calculations (i.e. 1976 US Standard Atmosphere).

As can be seen from Fig. 5, saturation and temperature corrections have the largest effect. We also checked the dependence of the retrieved CO$_2$ amount on the retrieved CH$_4$ (and vice versa). These dependences are small (even lower than the pressure dependence) and are therefore neglected.

Please note that at a fixed altitude seasonal variations of stratospheric temperature and pressure (and by this CO$_2$ number density) are typically less than about ±20 %. The effective corrections to be applied are therefore usually quite small, typically not larger than a few percent. The correction factors are derived from radiative transfer calculations and are therefore in principle as accurate as these calculations. The main uncertainties arise from (1) their calculation via scaled profiles and (2) the later interpolation of the database. Using scaled profiles is a valid approximation, considering that the vertical resolution is about 4.3 km, which is essentially determined by the vertical smoothing, and that most information is derived from altitudes close the tangent height.

The interpolation error is quite small (typically below 0.1 %) and could be further reduced by extension of the database. Overall, the contribution of the uncertainties of the correction factors to the error of the derived profiles is considered to be in the sub-percent range.

5 Results

5.1 Example profiles

The effect of the algorithm improvements can be seen in Fig. 6, which shows the resulting CH$_4$ on the left (both for version 3.3.6 and 4.5.2) and the CO$_2$ VMRs for an example measurement on the right (same orbit as in previous figures). For comparison, collocated data from ACE-FTS CH$_4$ and CarbonTracker CO$_2$ profiles are also shown. The ACE-FTS error bars represent the retrieval statistical fitting error.

The ONPD CH$_4$ profiles are in good agreement with the ACE-FTS data above about 20 km. Below this altitude, the previous product version 3.3.6 CH$_4$ drops off significantly, whereas the new version 4.5.2 product is still very close to the ACE-FTS results. The error of the SCIAMACHY V4.5.2 data is significantly lower than for V3.3.6. This is mainly due
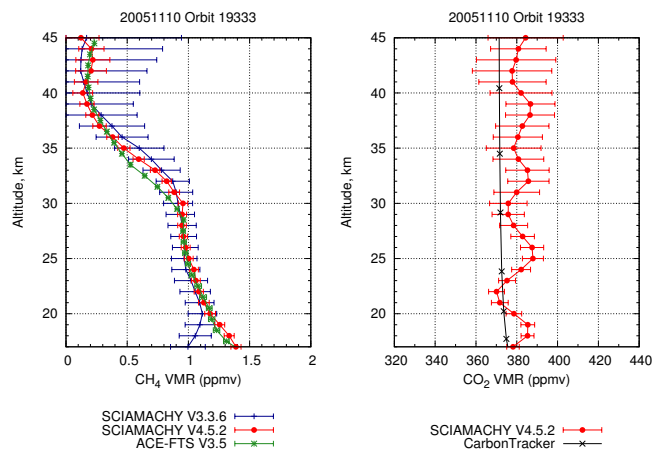
Figure 6. Example for resulting VMR profiles for CH₄ (left) and CO₂ (right). Red shows the results for the current product version (V4.5.2). For comparison, the CH₄ profile from the previous product version (V3.3.6) is also shown in the left plot in blue. Green (left) indicates collocated CH₄ profiles from ACE-FTS V3.5. Black (right) indicates the CO₂ profile from CarbonTracker (CT2013). Error bars denote the errors given in the products. No error is given for the CarbonTracker model data.

Figure 7. Top: time series of SCIAMACHY CH₄ VMRs at 30 km. Middle: time series of collocated MIPAS (blue), HALOE (grey) and ACE-FTS (green) CH₄ VMRs. Bottom: time series of CO₂ VMRs at 30 km. Red: SCIAMACHY data. Black: collocated CarbonTracker data.

to the correction factors applied to the errors as explained above.

For CO₂, there is no V3.3.6 product. The comparison of the new SCIAMACHY V4.5.2 CO₂ product with Carbon-Tracker model data shows a systematic positive offset of the SCIAMACHY data of about 10 ppmv above 25 km for this orbit; below this altitude the agreement is better. Especially at these lower altitudes, the SCIAMACHY data show a pronounced oscillation which is not expected from Carbon-Tracker data and larger than the estimated error of the SCIAMACHY product. This oscillation could already be observed in the derived correction factors (Fig. 4). It is probably a retrieval artefact and does not represent true CO₂ variations in the stratosphere. However, CarbonTracker is mainly designed to model tropospheric CO₂ and has only very few data points in the stratosphere (as can be seen from Fig. 6). Therefore no clear conclusion can be drawn at the moment; further investigations are needed.

5.2 Comparison with independent data sets

The complete SCIAMACHY occultation data set reaching from August 2002 until the end of the Envisat mission in April 2012 has been processed with the updated ONPD algorithm. From these, about 2000 orbits of reduced instrument performance (mainly related to instrument switch-offs or decontamination periods) have been excluded, resulting in more than 43 000 CH₄ and CO₂ profiles. In order to assess the quality of the derived SCIAMACHY ONPD CH₄ and CO₂ profiles, it is necessary to compare them with independent data.
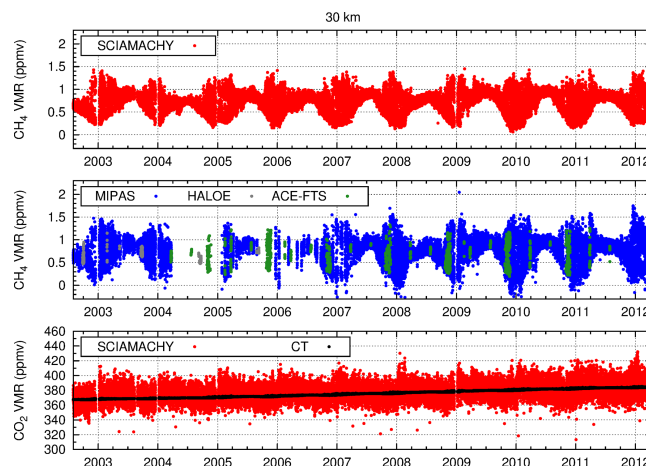
The SCIAMACHY methane data have been compared with results from ACE-FTS, HALOE and MIPAS. The vertical resolution of these data products is quite similar (ACE-FTS about 4 km, MIPAS about 2.5–7 km, HALOE about 2.5 km). This is why we did not consider differences in vertical resolution explicitly in the comparisons (e.g. by application of averaging kernels). This approach is consistent with the one used in Laeng et al. (2015), who state that the inclusion of averaging kernels in similar comparisons has an effect of only about 2 %. SCIAMACHY CO₂ profiles have been compared with data from ACE-FTS for altitudes below 25 km and with data from the CarbonTracker model (CT2013).

The top plot of Fig. 7 shows, as an example, a time series of the SCIAMACHY CH₄ data at 30 km altitude. In the middle figure, the corresponding collocated ACE-FTS, HALOE and MIPAS data are displayed. The bottom figure shows the SCIAMACHY and CarbonTracker CO₂ data sets. ACE-FTS CO₂ data are not included in this plot, because they are not available at this altitude.

The overall temporal behaviour of the different time series is quite similar. All CH₄ data sets show a large seasonal variation and a significant scatter, except for HALOE, where the seasonal coverage of the collocations is not sufficient to draw this conclusion. The variability is largest in winter/spring, due to the influence of the polar vortex (as already discussed in Noël et al., 2011). Both the SCIAMACHY and CT2013 CO₂ time series show a continuous increase with time (as expected from rising tropospheric CO₂), but the scatter in the SCIAMACHY data is much larger than in the model data. One possible explanation for this scatter is of course the error of the SCIAMACHY CO₂ data (which is about 10 ppmv at this altitude, see e.g. Fig. 6). On the other hand, Carbon-
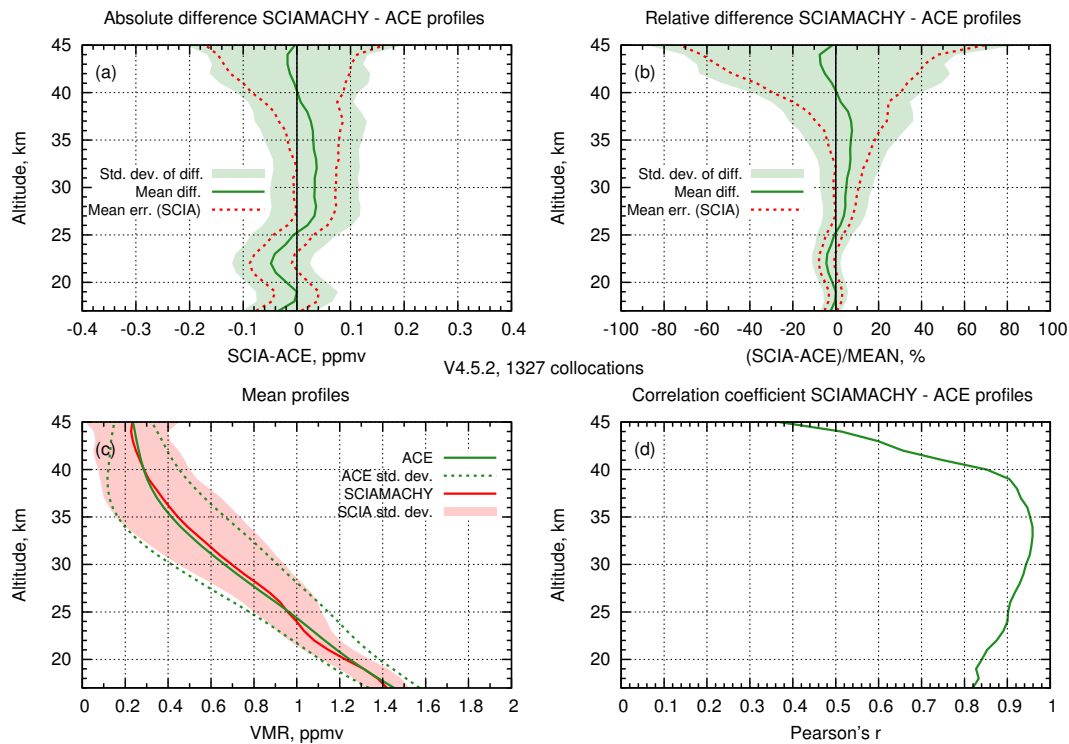
Figure 8. Comparison of retrieved SCIAMACHY CH$_4$ profiles (ONPD V4.5.2) with ACE-FTS data (V3.5). **(a)** Mean absolute difference (green) plus/minus one standard deviation (shaded area) and mean absolute error of SCIAMACHY data (dotted red line). **(b)** Mean relative difference (green) plus/minus one standard deviation (shaded area) and mean relative error of SCIAMACHY data (dotted red line). **(c)** Mean profiles and standard deviations (red: SCIAMACHY, green: ACE-FTS). **(d)** Correlation between SCIAMACHY and ACE-FTS data.

Tracker is a model which uses fully consistent information about the atmosphere, whereas e.g. pressure and temperature profiles used in the calculation of the SCIAMACHY VMRs are derived from the closest ECMWF data and thus never fully match the actual conditions.

Results from a more quantitative comparison between the different data sets is given in the following subsections.

5.2.1 Comparison with ACE-FTS CH$_4$

The results of the intercomparison between SCIAMACHY and ACE-FTS CH$_4$ are shown in Fig. 8. Overall, the two data sets agree within about 5–10 %. Between 25 and 40 km the SCIAMACHY data are typically higher than ACE-FTS data; the mean offset over all altitudes between 17 and 45 km is about 3 %. This is within the expected accuracy of the products and better than the mean difference between the previous product version and ACE-FTS V2.2 data which was about 10 % (Noël et al., 2011). The differences show a small oscillation with altitude (especially below about 25 km), which might be related to the onion peeling approach as discussed above. The mean profiles (shown in Fig. 8c) indicate that this oscillation of the differences is caused by the SCIAMACHY data. The estimated mean error of the SCIAMACHY CH$_4$ product (single profile at 1 km vertical sampling) is about

0.05 ppmv between 17 and 35 km (which is about two times smaller than the standard deviation of the difference between the two data sets) and increasing to about 0.1 ppmv for higher altitudes. Especially below 40 km the correlation between SCIAMACHY and ACE-FTS CH$_4$ (Fig. 8d) is high, reaching about 0.95 between 30 and 35 km. This indicates that both instruments see a similar temporal variability in CH$_4$, which is also in line with the similar standard deviations shown in Fig. 8c.

5.2.2 Comparison with HALOE

The results of the comparison between SCIAMACHY and HALOE CH$_4$ profiles are shown in Fig. 9. Above 20 km, the relative and absolute differences are very similar to those from the comparison with ACE-FTS (Fig. 8). Between about 25 and 40 km and at the lowest altitudes, SCIAMACHY VMRs are up to about 10 % higher than those from HALOE; the overall agreement is quite good above 40 km. Some oscillation is visible in the differences and the mean SCIA-MACHY profile. The correlation between SCIAMACHY and HALOE CH$_4$ is somewhat smaller than between SCIA-MACHY and ACE-FTS, which is probably related to the specific temporal sampling (see top plot of Fig. 7), resulting in
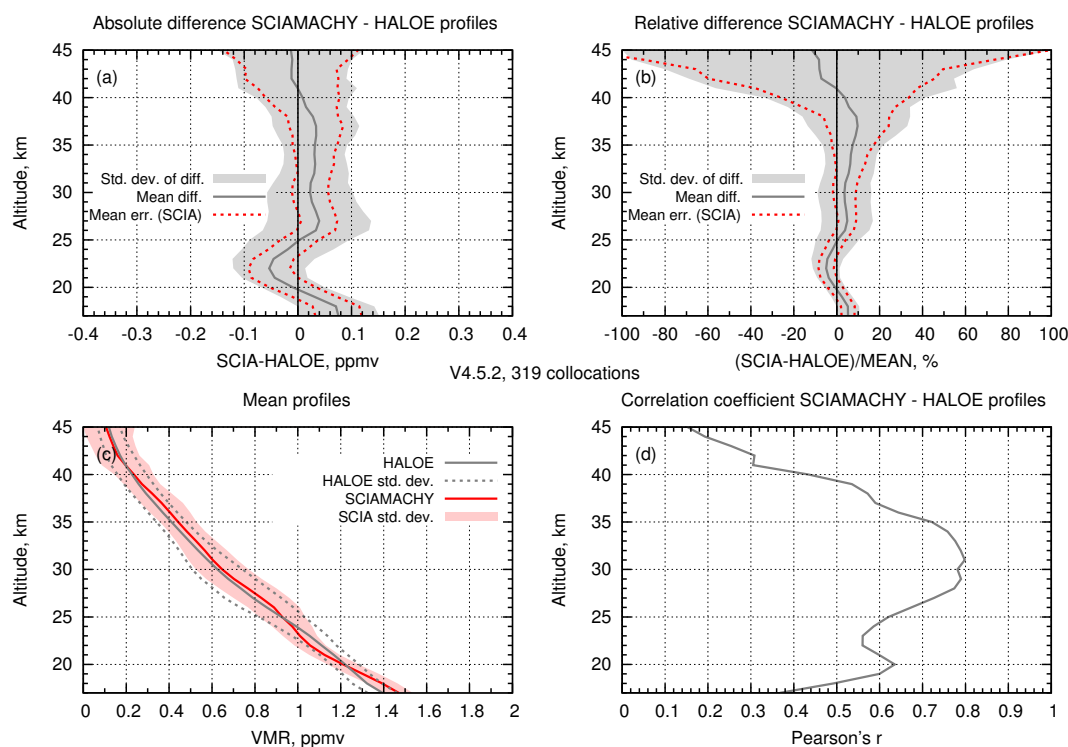
Figure 9. Same as Fig. 8, but for comparison of retrieved SCIAMACHY CH$_4$ profiles (ONPD V4.5.2, red) with HALOE v19 sunset data (grey).

less variability. This is in line with the smaller standard deviations of the mean profiles.

5.2.3 Comparison with MIPAS

Figure 10 shows the results of the intercomparison between SCIAMACHY and MIPAS CH$_4$ profiles in a similar way to the comparisons with ACE-FTS and HALOE. As can be seen from this plot, the systematic differences between SCIA-MACHY and MIPAS are near zero above 25 km. Below this altitude, the deviation between SCIAMACHY and MIPAS data increases with decreasing altitude, reaching about -0.2 ppmv (10–15 %) at 17 km. This negative bias of SCIA-MACHY towards MIPAS is in line with the about 0.2 ppmv positive bias of MIPAS in this altitude range (Laeng et al., 2015). Especially at these lower altitudes the correlation between MIPAS and SCIAMACHY is somewhat smaller than between ACE-FTS and SCIAMACHY. The maximum correlation occurs at around 30 km, reaching almost 0.9.

5.2.4 Comparison with ACE-FTS CO$_2$ data

The results of the comparison between the ONPD CO$_2$ data and the ACE-FTS CO$_2$ data, derived using the algorithm by Sioris et al. (2014), are shown in Fig. 11. The agreement between SCIAMACHY and ACE-FTS data is within about 2 %. The small increase in the ACE-FTS CO$_2$ above about

22 km is related to a high bias in the ACE-FTS data, due to a HDO interference which is not properly taken into account in this product version. The correlation is quite low, but this can be expected, because the expected natural variability in CO$_2$ is typically of the same magnitude as the errors of the individual profiles. The vertical range where the data sets overlap (17–24 km) is about the typical wavelength of the vertical oscillations seen in the SCIAMACHY profiles (or even smaller), such that the differences are dominated by the oscillations in the SCIAMACHY data. The fact that such oscillations are not seen in the ACE-FTS data is a further indication that these are a SCIAMACHY retrieval artefact.

5.2.5 Comparison with CarbonTracker

The ONPD CO$_2$ profiles have been compared with the CT2013 data derived from the CarbonTracker model (Peters et al., 2007). The results of the CO$_2$ comparison are shown in Fig. 12. As for CH$_4$, a variation of the differences with altitude can be clearly seen, similar to the example shown in Fig. 6. Except for these oscillations with altitude, there is no apparent altitude-independent systematic bias between SCIAMACHY ONPD CO$_2$ and Carbon-Tracker, meaning that such a bias would be significantly lower than the amplitude of the oscillations of about 10 ppmv (3 %). The mean error of the SCIAMACHY CO$_2$ product is about 4 ppmv (1 %) at 17 km, increasing to about 16 ppmv
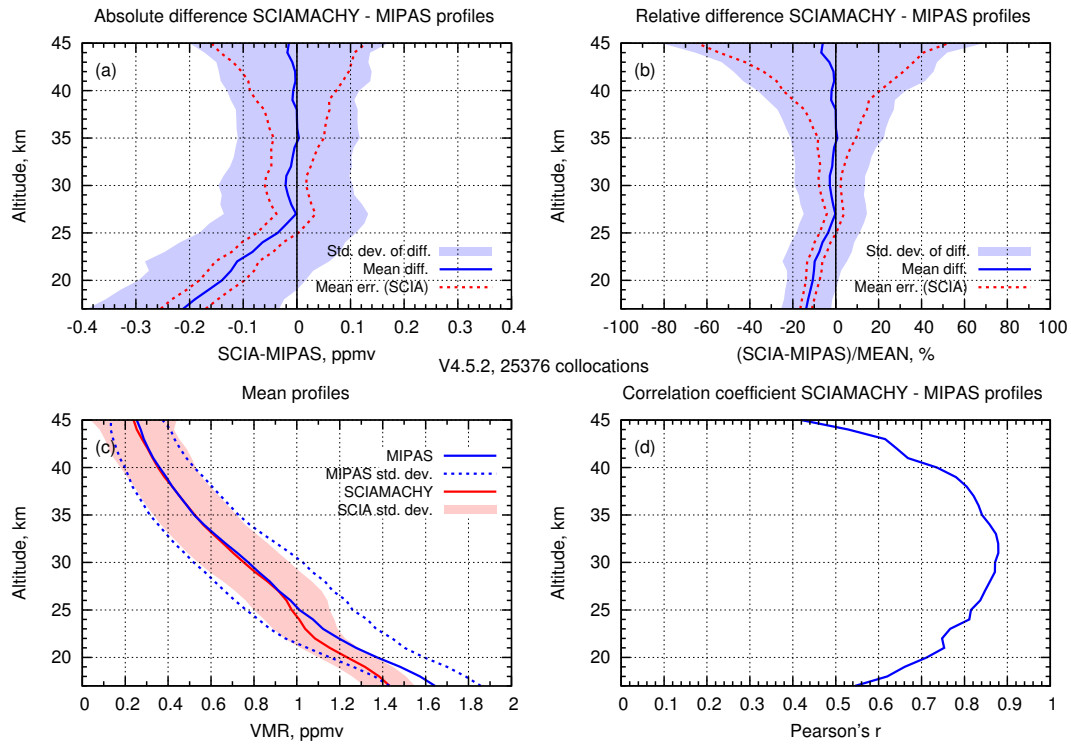
Figure 10. Same as Fig. 8, but for comparison of retrieved SCIAMACHY CH$_4$ profiles (ONPD V4.5.2, red) with MIPAS data (blue).
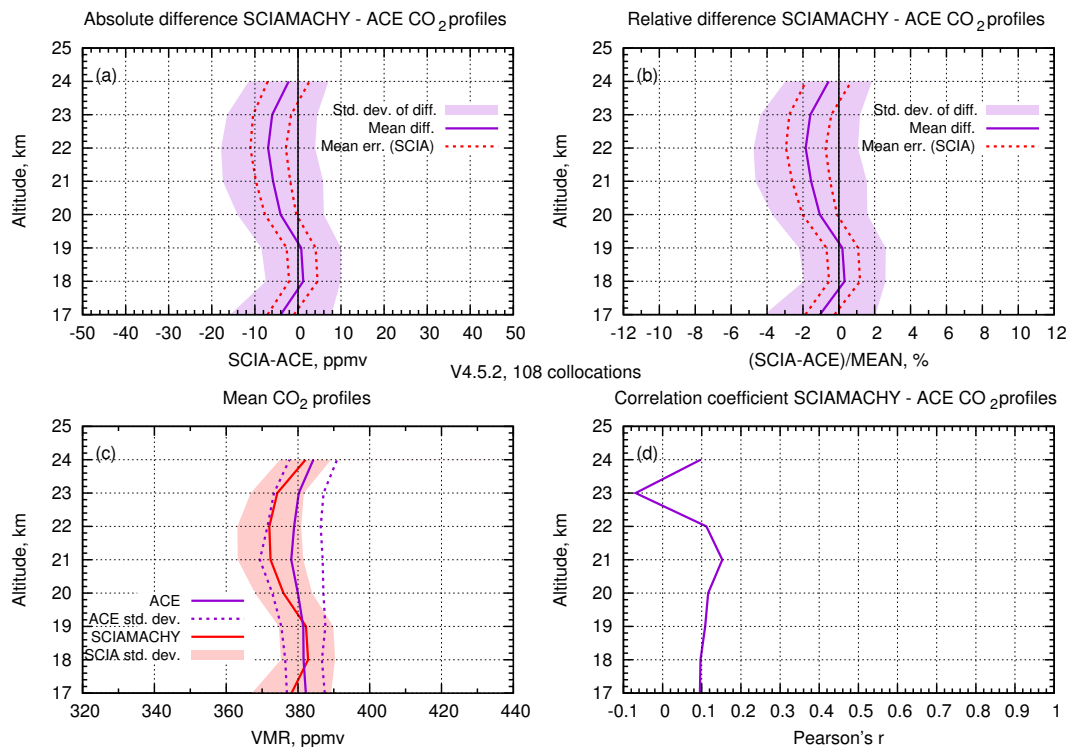

Figure 11. Same as Fig. 8, but for comparison of retrieved SCIAMACHY CO$_2$ profiles (ONPD V4.5.2, red) with ACE-FTS CO$_2$ after Sioris et al. (2014) (violet).
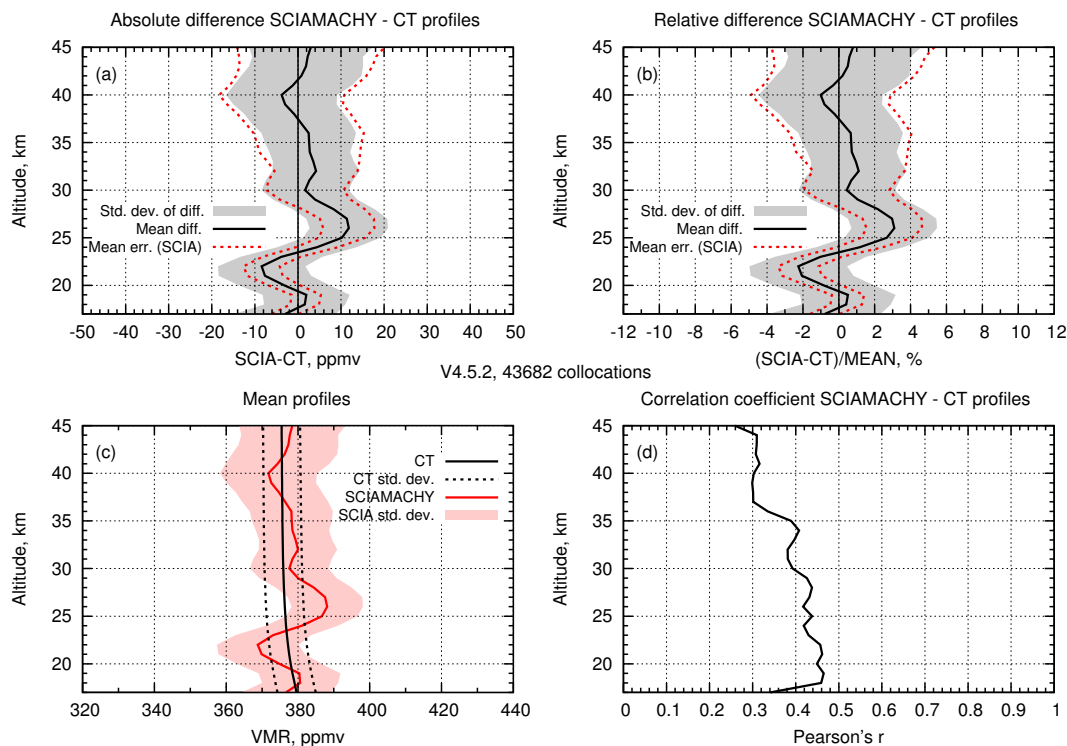
Figure 12. Same as Fig. 8, but for comparison of retrieved SCIAMACHY CO_2 profiles (ONPD V4.5.2, red) with CarbonTracker CT2013 data (black).

(4 %) at 45 km. At higher altitudes the error is even slightly larger than the standard deviation of the difference between both data sets, which is over the whole altitude range about 10–15 ppmv, i.e. less than about 4 %. This indicates that above about 32 km the estimated error of the CO_2 profiles might – despite the additional corrections performed after the retrieval as described above – still be overestimated. Probably because of the generally low variability of stratospheric CO_2 VMRs and the larger variability of the SCIAMACHY data (see standard deviations in Fig. 12c), the maximum correlation with CarbonTracker CO_2 is only about 0.45.

5.3 Time series of SCIAMACHY CH₄ and CO₂ data

To reduce the impact of the scatter between the individual measurement results, daily averages of the SCIAMACHY VMR data have been computed. These are based on up to 15 individual profiles at different geographical longitudes but – because of the sun-fixed Envisat orbit – at almost the same geographical latitude, so these are essentially zonal means.

The resulting time series for daily averaged CH₄ and CO₂ are shown in Fig. 13. For each gas, a contour plot shows the change of the VMRs with time and altitude, together with the average tropopause height derived from ECMWF data. Above the contour plots the variation of the geographical latitudes of the SCIAMACHY measurements with time is displayed.

The time series for CH₄ (Fig. 13a) shows a clear variation with latitude and/or tropopause height. This variation is very similar to that observed for the previous product version (Noël et al., 2011) and is attributed to the direct and non-separable relation between time and latitude of the solar occultation measurements imposed by the sun-fixed Envisat orbit.

In Fig. 13b the complete SCIAMACHY time series of daily averaged CO_2 profiles is given. This figure shows a similar variation of the CO_2 VMRs with latitude and/or tropopause height as observed for CH₄. In addition, there is a pronounced variation of the CO_2 VMRs with altitude. Highest CO_2 VMRs occur between about 25 and 30 km. As mentioned before, this variation, which was also visible in the comparison with CarbonTracker (Fig. 12), is assumed to be related to the ONPD retrieval, but this issue is still under investigation. Furthermore, a general increase of stratospheric CO_2 over time is observed, which is expected as tropospheric CO_2 also increases with time.

5.4 Preliminary trend analysis

The ONPD method uses the solar transmittance as input, which is computed from the ratio of two radiance measurements at different altitudes. Furthermore, a polynomial is fitted to the data. Therefore, the ONPD retrieval is very insensitive to systematic instrumental errors (like degradation) or
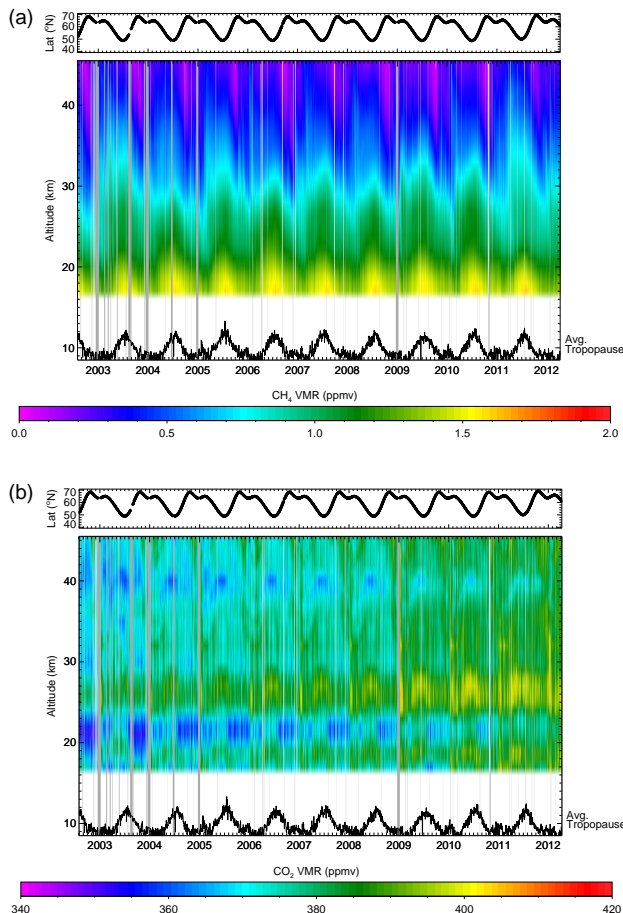
Figure 13. Time series of daily averaged CH$_4$ (**a**) and CO$_2$ (**b**) profiles August 2002–April 2012. Areas with reduced instrument performance (decontaminations, switch-off, etc.) are masked out by grey bars. The lower, black curve shows average tropopause height derived from ECMWF data. Top graph of each sub-figure shows the tangent latitude of observation.

uncertainties in the radiometric calibration. This makes the SCIAMACHY ONPD data especially suited for trend analyses.

However, as shown in the previous sections, the temporal variability is large and the data seem to be affected by a currently unexplained systematic effect resulting in an unexpected vertical oscillation in the derived profiles. For the estimation of trends from the SCIAMACHY data set, we therefore first determine monthly anomaly profiles by the following procedure:

1. Monthly average VMR profiles are computed from the daily average data shown in Fig. 13.

2. For each month, an average profile is computed resulting in a mean profile (e.g. all January profiles are averaged to get a mean January profile for the time series).
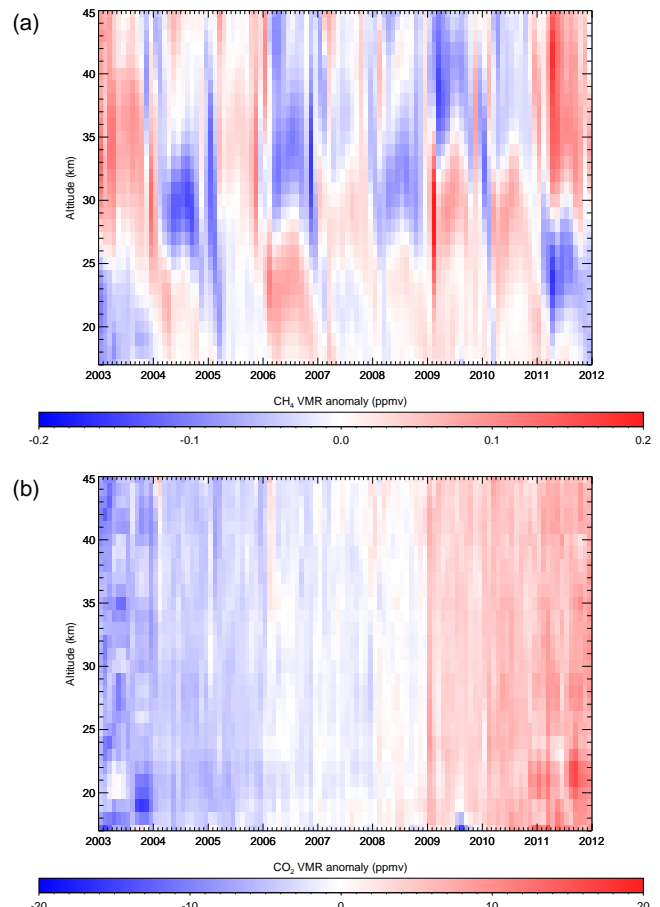

Figure 14. Time series of CH$_4$ (**a**) and CO$_2$ (**b**) monthly VMR anomaly profiles January 2003–December 2011.

3. The mean profile for one month is then subtracted from all corresponding profiles (e.g. the mean January profile is subtracted from all individual January profiles).

All these operations are performed independently for each altitude for all data from January 2003 to December 2011. Retrieved profiles from August to December 2002 and January to April 2012 have been excluded to avoid different weighting of different seasons.

The resulting VMR anomalies are less affected by noise and short-term variability. Furthermore, regular seasonal/latitudinal effects have been removed from the data by this procedure. Since the observed vertical oscillations are very stable with time, they are also essentially eliminated. This can be seen from Fig. 14, which shows time series of the resulting VMR anomalies for both CH$_4$ and CO$_2$.

The CO$_2$ anomaly plot (Fig. 14b) is especially much smoother than the corresponding daily data (Fig. 13b). Except for some small regions, e.g. around 20 km at the end of 2003 and 2011, a continuous increase with time is observed at all altitudes. There are also indications for some remaining instrumental influences, e.g. due to thermal instabilities after
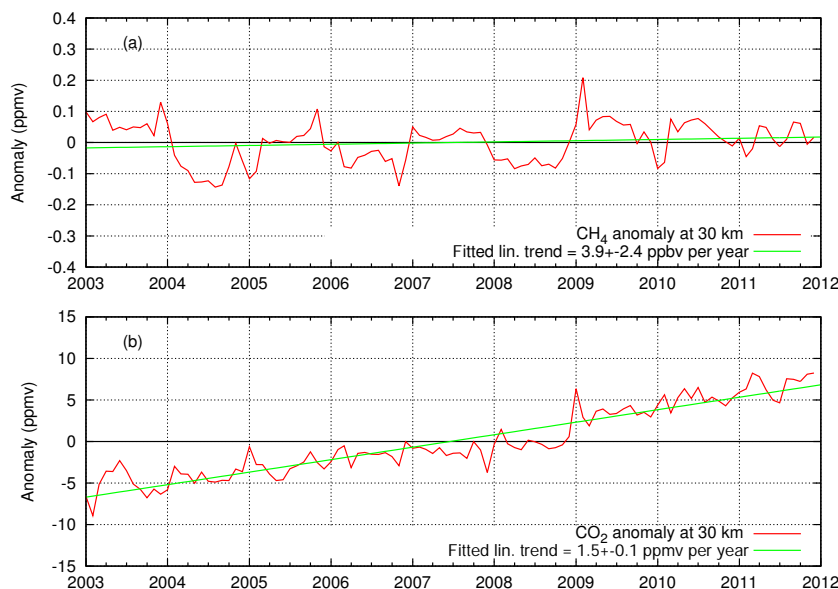
Figure 15. Time series of SCIAMACHY CH_4 **(a)** and CO_2 **(b)** VMR anomalies at 30 km. Red lines show the daily averaged data. Green lines show the linear trend.

a decontamination like in January 2009. The lower CO_2 values at the lowest altitudes in the second half of 2009 are most likely due to a remnant sensitivity of the retrieval to increased aerosol, related to the eruption of the Sarychev volcano on 12 June 2009 (see e.g. Kravitz et al., 2011).

Furthermore, the variability in the derived CO_2 anomalies is somewhat higher in 2003 (before the update of the Envisat on-board orbit model) and after the Envisat orbit change end of 2010. This is because during these times the vertical sampling pattern of the SCIAMACHY solar occultations measurements was slightly different such that (systematically) spectra at other altitudes were selected as input for the retrieval. The additional spatial and temporal variations in the anomalies at the beginning and the end of the mission are therefore an estimate of the sensitivity of the ONPD retrieval to the vertical sampling. The fact that the vertical distribution can be influenced by the sampling of the measurement data is also an indication that the observed unexpected vertical oscillations in the CO_2 data may be a retrieval artefact.

In contrast, the CH_4 anomalies (Fig. 14a) show no clear trend, but some distinct features. For example, the year-to-year variability of the polar vortex can be seen from the higher variability in the CH_4 anomalies during winter/spring time. Due to the downward transport of upper stratospheric/mesospheric air CH_4 VMRs inside the vortex are usually lower than outside the vortex. The average monthly CH_4 profile depends therefore on the number of contributing profiles from inside/outside the vortex. For example in February 2009, there are (based on potential vorticity derived from ECMWF data) only very few profiles located inside the vortex in contrast to other years, which results in a positive anomaly for this month.

In addition, there is a pattern of alternating positive and negative anomalies occurring around 30 km before 2009 and somewhat above and below after that time. This pattern has an approximate frequency of two years, therefore we assume that it is caused by transport effects related to the quasi-biennial oscillation (QBO), see e.g. Baldwin et al. (2001).

It is probably worthwhile to look deeper into these effects during further studies. However, in the present work we only want to show that such information is contained in the ONPD data, which makes them useful for stratospheric studies.

From the monthly anomalies we obtain a linear trend by simply fitting a straight line to the data for each altitude. As an example, Fig. 15 shows time series of CH_4 and CO_2 monthly anomalies at 30 km altitude and the corresponding fit results. For CO_2 a significant positive trend of 1.5 ppmv year⁻¹ is obtained at this altitude. No clear CH_4 trend is visible by eye; the fit results in a small but insignificant positive trend which is much smaller than the variability in the data.

Figure 16 shows the derived 2003–2011 linear trends as a function of altitude on an 1 km grid. The left panel of this figure shows the calculated altitude-dependent trends of CH_4, the right panel those of CO_2. As can be seen from the 2σ ranges, all of the CO_2 trends are significantly different from zero, whereas for CH_4 only trends below about 20 km are usually larger than two times their error. The CH_4 trends show an oscillation with altitude which seems non-erratic but is within the estimated error of the trends.

Especially because of the very specific temporal and spatial sampling of the SCIAMACHY solar occultation measurements, a quantitative comparison of the derived ONPD trends with other data sets is in general not easy. However,
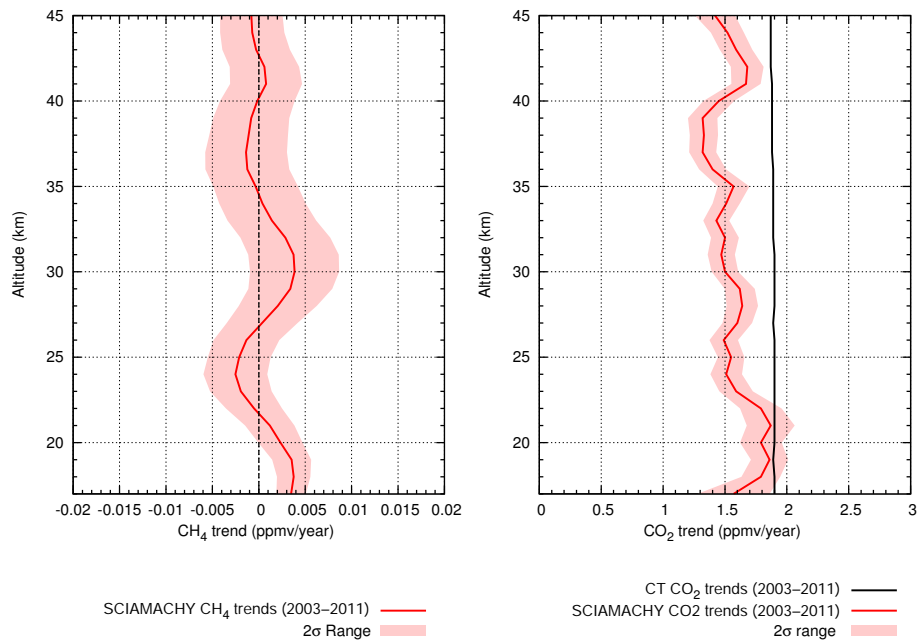
Figure 16. Calculated trends of CH$_4$ (left, red curve) and CO$_2$ (right, red curve) VMRs 2003 to 2011 as function of altitude. Shaded areas denote the 2σ error range of the derived trends. For comparison, the corresponding trend derived from CarbonTracker CT2013 data is also shown in black. Note that the 2σ range for CarbonTracker is smaller than the thickness of the trend line and therefore not visible in the plot.

the ONPD CH$_4$ trends below 20 km of about 3 ppbv year^{-1} are roughly in line with total column trends derived from nadir measurements. For example, Schneising et al. (2011) determined from SCIAMACHY data a total dry-air column-average CH$_4$ linear change in the Northern Hemisphere of about 8 ppbv year^{-1} between 2007 and 2009 and an almost zero trend before. Frankenberg et al. (2011) report – also based on SCIAMACHY data – an increase of about 20–25 ppbv total dry-air column-average CH$_4$ between 2003 and 2009 at northern latitudes.

The ONPD CO$_2$ trends depicted in the right plot of Fig. 16 vary between about 1.3 and 1.9 ppmv year^{-1}. For comparison, CT2013 trends are also shown. The CarbonTracker trends have been calculated in the same way as the SCIA-MACHY CO$_2$ trends, i.e. based on monthly anomalies derived from the collocated profiles. The SCIAMACHY CO$_2$ trends are somewhat lower than the corresponding CarbonTracker changes of about 1.9 ppmv year^{-1} and show a slight decrease with altitude which is less pronounced in the CT2013 trends. Some oscillations with altitude are also visible in the SCIAMACHY CO$_2$ trends, but these are much smaller than the trends. For the CO$_2$ total dry-air column-average Schneising et al. (2013) determined a northern hemispheric trend of about 1.8 ppmv year^{-1} between 2003 and 2009, which is – considering different temporal and spatial sampling, different altitudinal ranges and different ways of calculating the trend – consistent with the lower stratospheric values resulting from the ONPD data.

6 Conclusions

The SCIAMACHY ONPD retrieval has been further developed in the context of the ESA GHG-CCI project, resulting in improved CH$_4$ stratospheric profiles now covering the altitude range between 17 and 45 km. Furthermore, the first SCIAMACHY CO$_2$ stratospheric profiles have been obtained.

The complete SCIAMACHY time series has been processed, resulting in a stratospheric CH$_4$ and CO$_2$ data set (V4.5.2) covering the time interval from August 2002 to April 2012. Because of the sun-fixed orbit of Envisat, the SCIAMACHY solar occultation measurements are restricted to latitudes between about 50 and 70° N. However, measurements of the stratospheric distribution of greenhouse gases are generally sparse. Therefore the new SCIAMACHY data sets, which cover almost ten years, can provide valuable information about stratospheric changes.

Intercomparisons with correlative data (ACE-FTS, HALOE and MIPAS CH$_4$; ACE-FTS and CT2013 CO$_2$) indicate an accuracy of the new products of about 5–10 % for CH$_4$ and 2–3 % for CO$_2$. At most altitudes, this is in fact similar to or even better than the estimated mean (statistical) error of the single profile products. However, at least for CO$_2$ there are indications that the error at altitudes above about 30 km is still overestimated.

First estimates of CH$_4$ and CO$_2$ trends have been derived from the SCIAMACHY ONPD time series (2003–2011). Above 20 km no significant CH$_4$ trends are observed.

At the lowest altitude (17 km) a small CH$_4$ trend of about 3 ppbv year^{-1} has been determined.

The derived CO$_2$ trends are significant at all altitudes and on the order of about 1.7 ppmv year^{-1}, slightly varying with altitudes between 1.3 ppmv year^{-1} (at 39 km) and 1.9 ppmv year^{-1} (at 21 km).

Considering the specific spatial and temporal sampling of the SCIAMACHY occultation data, these trends are in reasonable agreement with total dry-air column-average trends of CH$_4$ and CO$_2$ obtained from SCIAMACHY.

The main issue to be resolved in the future is an unexpected vertical oscillation in the resulting CH$_4$ and CO$_2$ profiles. These oscillations are currently considered to be the most limiting factor for the accuracy of the ONPD products and need further investigation.

A possible way forward in this context is to use the ONPD method to derive pressure and temperature data from SCIAMACHY solar occultation measurements in the atmospheric O$_2$(A) band around 760 nm. These data could then be used in the CH$_4$ and CO$_2$ retrievals instead of the ECMWF data. This way, potential systematic errors might be cancelled and the ONPD data products would be less dependent on ECMWF data. However, this would require high-quality ONPD pressure and temperature products, which are not yet available. This will be subject to future studies.

Especially for CO$_2$, another option to be followed in the future is the application of alternative retrieval algorithms. Possible candidates for this would be a two-step approach used e.g. in GOMOS stellar occultation retrievals (Kyrölä et al., 2010) or the use of a full optimal estimation-based retrieval, including online radiative transfer calculations to the SCIAMACHY solar occultation data (see e.g. Bramstedt et al., 2009). The latter kind of retrieval is in particular computationally much more expensive, but vertical oscillations can be better handled via appropriate regularisation and the retrieval is less sensitive to non-linear effects arising from e.g. saturation or varying temperature and pressure.

Edited by: C. von Savigny

References

Baldwin, M. P., Gray, L. J., Dunkerton, T. J., Hamilton, K., Haynes, P. H., Randel, W. J., Holton, J. R., Alexander, M. J., Hirota, I., Horinouchi, T., Jones, D. B. A., Kinnersley, J. S., Marquardt, C., Sato, K., and Takahashi, M.: The quasi-biennial oscillation, Rev. Geophys., 39, 179–229, doi:10.1029/1999RG000073, 2001.

Beagley, S. R., Boone, C. D., Fomichev, V. I., Jin, J. J., Semeniuk, K., McConnell, J. C., and Bernath, P. F.: First multi-year occultation observations of CO$_2$ in the MLT by ACE satellite: observations and analysis using the extended CMAM, Atmos. Chem. Phys., 10, 1133–1153, doi:10.5194/acp-10-1133-2010, 2010.

Bernath, P. F., McElroy, C. T., Abrams, M. C., Boone, C. D., Butler, M., Camy-Peyret, C., Carleer, M., Clerbaux, C., Coheur, P.-F., Colin, R., DeCola, P., DeMazière, M., Drummond, J. R., Dufour, D., Evans, W. F. J., Fast, H., Fussen, D., Gilbert, K., Jennings, D. E., Llewellyn, E. J., Lowe, R. P., Mahieu, E., McConnell, J. C., McHugh, M., McLeod, S. D., Michaud, R., Midwinter, C., Nassar, R., Nichitiu, F., Nowlan, C., Rinsland, C. P., Rochon, Y. J., Rowlands, N., Semeniuk, K., Simon, P., Skelton, R., Sloan, J. J., Soucy, M.-A., Strong, K., Tremblay, P., Turnbull, D., Walker, K. A., Walkty, I., Wardle, D. A., Wehrle, V., Zander, R., and Zou, J.: Atmospheric Chemistry Experiment (ACE): mission overview, Geophys. Res. Lett., 32, L15S01, doi:10.1029/2005GL022386, 2005.

Boone, C. D., Nassar, R., Walker, K. A., Rochon, Y., McLeod, S. D., Rinsland, C. P., and Bernath, P. F.: Retrievals for the atmospheric chemistry experiment Fourier-transform spectrometer, Appl. Optics, 44, 7218–7231, 2005.

Boone, C. D., Walker, K. A., and Bernath, P. F.: Version 3 retrievals for the atmospheric chemistry experiment fourier transform spectrometer (ACE-FTS), in: The Atmospheric Chemistry Experiment ACE at 10: A Solar Occultation Anthology, edited by: Bernath, P. F., A. Deepak Publishing, Hampton, Virginia, USA, 103–127, 2013.

Bovensmann, H., Burrows, J. P., Buchwitz, M., Frerick, J., Noël, S., Rozanov, V. V., Chance, K. V., and Goede, A. H. P.: SCIAMACHY – mission objectives and measurement modes, J. Atmos. Sci., 56, 127–150, 1999.

Bramstedt, K., Amekudzi, L. K., Rozanov, A., Bovensmann, H., and Burrows, J.: SCIAMACHY solar occultation: ozone and NO$_2$ profiles 2002–2007, in: New Horizons in Occultation Research, edited by: Steiner, A., Foelsche, U., Pirscher, B., and Kirchengast, G., Springer Berlin Heidelberg, 79–86, 2009.

Bramstedt, K., Noël, S., Bovensmann, H., Gottwald, M., and Burrows, J. P.: Precise pointing knowledge for SCIAMACHY solar occultation measurements, Atmos. Meas. Tech., 5, 2867–2880, doi:10.5194/amt-5-2867-2012, 2012.

Burrows, J. P., Weber, M., Buchwitz, M., Rozanov, V., Ladstätter-Weißenmayer, A., Richter, A., de Beek, R., Hoogen, R., Bramstedt, K., Eichmann, K.-U., Eisinger, M., and Perner, D.: The Global Ozone Monitoring Experiment (GOME): mission concept and first scientific results, J. Atmos. Sci., 56, 151–175, 1999.

Coldewey-Egbers, M., Weber, M., Lamsal, L. N., de Beek, R., Buchwitz, M., and Burrows, J. P.: Total ozone retrieval from GOME UV spectral data using the weighting function DOAS approach, Atmos. Chem. Phys., 5, 1015–1025, doi:10.5194/acp-5-1015-2005, 2005.

Dee, D. P., Uppala, S. M., Simmons, A. J., Berrisford, P., Poli, P., Kobayashi, S., Andrae, U., Balmaseda, M. A., Balsamo, G., Bauer, P., Bechtold, P., Beljaars, A. C. M., van de Berg, L., Bidlot, J., Bormann, N., Delsol, C., Dragani, R., Fuentes, M., Geer, A. J., Haimberger, L., Healy, S. B., Hersbach, H., Hólm, E. V., Isaksen, L., Kållberg, P., Köhler, M., Matricardi, M., McNally, A. P., Monge-Sanz, B. M., Morcrette, J.-J., Park, B.-K., Peubey, C., de Rosnay, P., Tavolato, C., Thépaut, J.-N., and Vitart, F.: The ERA-Interim reanalysis: configuration and performance of the data assimilation system, Q. J. Roy. Meteor. Soc., 137, 553–597, doi:10.1002/qj.828, 2011.

De Mazière, M., Vigouroux, C., Bernath, P. F., Baron, P., Blumenstock, T., Boone, C., Brogniez, C., Catoire, V., Coffey, M., Duchatelet, P., Griffith, D., Hannigan, J., Kasai, Y., Kramer, I., Jones, N., Mahieu, E., Manney, G. L., Piccolo, C., Randall, C., Robert, C., Senten, C., Strong, K., Taylor, J., Tétard, C., Walker, K. A., and Wood, S.: Validation of ACE-FTS v2.2 methane profiles from the upper troposphere to the lower mesosphere, Atmos. Chem. Phys., 8, 2421–2435, doi:10.5194/acp-8-2421-2008, 2008.

Emmert, J. T., Stevens, M. H., Bernath, P. F., Drob, D. P., and Boone, C. D.: Observations of increasing carbon dioxide concentration in Earth's thermosphere, Nat. Geosci., 5, 868–871, doi:10.1038/ngeo1626, 2012.

Fischer, H., Birk, M., Blom, C., Carli, B., Carlotti, M., von Clarmann, T., Delbouille, L., Dudhia, A., Ehhalt, D., Endemann, M., Flaud, J. M., Gessner, R., Kleinert, A., Koopman, R., Langen, J., López-Puertas, M., Mosner, P., Nett, H., Oelhaf, H., Perron, G., Remedios, J., Ridolfi, M., Stiller, G., and Zander, R.: MIPAS: an instrument for atmospheric and climate research, Atmos. Chem. Phys., 8, 2151–2188, doi:10.5194/acp-8-2151-2008, 2008.

Foucher, P. Y., Chédin, A., Dufour, G., Capelle, V., Boone, C. D., and Bernath, P.: Technical Note: Feasibility of CO$_2$ profile retrieval from limb viewing solar occultation made by the ACE-FTS instrument, Atmos. Chem. Phys., 9, 2873–2890, doi:10.5194/acp-9-2873-2009, 2009.

Foucher, P. Y., Chédin, A., Armante, R., Boone, C., Crevoisier, C., and Bernath, P.: Carbon dioxide atmospheric vertical profiles retrieved from space observation using ACE-FTS solar occultation instrument, Atmos. Chem. Phys., 11, 2455–2470, doi:10.5194/acp-11-2455-2011, 2011.

Frankenberg, C., Aben, I., Bergamaschi, P., Dlugokencky, E. J., van Hees, R., Houweling, S., van der Meer, P., Snel, R., and Tol, P.: Global column-averaged methane mixing ratios from 2003 to 2009 as derived from SCIAMACHY: trends and variability, J. Geophys. Res., 116, D04302, doi:10.1029/2010JD014849, 2011.

Gottwald, M. and Bovensmann, H. (Eds.): SCIAMACHY – Exploring the Changing Earth's Atmosphere, Springer, Dordrecht, Heidelberg, London, New York, doi:10.1007/978-90-481-9896-2, 2011.

Kravitz, B., Robock, A., Bourassa, A., Deshler, T., Wu, D., Mattis, I., Finger, F., Hoffmann, A., Ritter, C., Bitar, L., Duck, T. J., and Barnes, J. E.: Simulation and observations of stratospheric aerosols from the 2009 Sarychev volcanic eruption, J. Geophys. Res., 116, D18211, doi:10.1029/2010JD015501, 2011.

Kuze, A., Suto, H., Nakajima, M., and Hamazaki, T.: Thermal and near infrared sensor for carbon observation Fourier-transform spectrometer on the Greenhouse Gases Observing Satellite for greenhouse gases monitoring, Appl. Optics, 48, 6716–6733, 2009.

Kyrölä, E., Tamminen, J., Sofieva, V., Bertaux, J. L., Hauchecorne, A., Dalaudier, F., Fussen, D., Vanhellemont, F., Fanton d'Andon, O., Barrot, G., Guirlet, M., Mangin, A., Blanot, L., Fehr, T., Saavedra de Miguel, L., and Fraisse, R.: Retrieval of atmospheric parameters from GOMOS data, Atmos. Chem. Phys., 10, 11881–11903, doi:10.5194/acp-10-11881-2010, 2010.

Laeng, A., Plieninger, J., von Clarmann, T., Grabowski, U., Stiller, G., Eckert, E., Glatthor, N., Haenel, F., Kellmann, S., Kiefer, M., Linden, A., Lossow, S., Deaver, L., Engel, A., Hervig, M., Levin, I., McHugh, M., Noël, S., Toon, G., and Walker, K.: Validation of MIPAS IMK/IAA methane profiles, Atmos. Meas. Tech., 8, 5251–5261, doi:10.5194/amt-8-5251-2015, 2015.

Noël, S., Bramstedt, K., Rozanov, A., Bovensmann, H., and Burrows, J. P.: Water vapour profiles from SCIAMACHY solar occultation measurements derived with an onion peeling approach, Atmos. Meas. Tech., 3, 523–535, doi:10.5194/amt-3-523-2010, 2010.

Noël, S., Bramstedt, K., Rozanov, A., Bovensmann, H., and Burrows, J. P.: Stratospheric methane profiles from SCIAMACHY solar occultation measurements derived with onion peeling DOAS, Atmos. Meas. Tech., 4, 2567–2577, doi:10.5194/amt-4-2567-2011, 2011.

Park, J. H., Russell, J. M., Gordley, L. L., Drayson, S. R., Benner, D. C., McInerney, J. M., Gunson, M. R., Toon, G. C., Sen, B., Blavier, J.-F., Webster, C. R., Zipf, E. C., Erdman, P., Schmidt, U., and Schiller, C.: Validation of Halogen Occultation Experiment CH$_4$ measurements from the UARS, J. Geophys. Res., 101, 10183–10203, doi:10.1029/95JD02736, 1996.

Payan, S., Camy-Peyret, C., Oelhaf, H., Wetzel, G., Maucher, G., Keim, C., Pirre, M., Huret, N., Engel, A., Volk, M. C., Kuellmann, H., Kuttippurath, J., Cortesi, U., Bianchini, G., Mencaraglia, F., Raspollini, P., Redaelli, G., Vigouroux, C., De Mazière, M., Mikuteit, S., Blumenstock, T., Velazco, V., Notholt, J., Mahieu, E., Duchatelet, P., Smale, D., Wood, S., Jones, N., Piccolo, C., Payne, V., Bracher, A., Glatthor, N., Stiller, G., Grunow, K., Jeseck, P., Te, Y., and Butz, A.: Validation of version-4.61 methane and nitrous oxide observed by MIPAS, Atmos. Chem. Phys., 9, 413–442, doi:10.5194/acp-9-413-2009, 2009.

Perner, D. and Platt, U.: Detection of nitrous acid in the atmosphere by differential optical absorption, Geophys. Res. Lett., 6, 917–920, 1979.

Peters, W., Jacobson, A. R., Sweeney, C., Andrews, A. E., Conway, T. J., Masarie, K., Miller, J. B., Bruhwiler, L. M. P., Pétron, G., Hirsch, A. I., Worthy, D. E. J., van der Werf, G. R., Randerson, J. T., Wennberg, P. O., Krol, M. C., and Tans, P. P.: An atmospheric perspective on North American carbon dioxide exchange: CarbonTracker, P. Natl. Acad. Sci. USA, 104, 18925–18930, doi:10.1073/pnas.0708986104, 2007.

Rozanov, V. V., Rozanov, A. V., Kokhanovsky, A. A., and Burrows, J. P.: Radiative transfer through terrestrial atmosphere and

ocean: software package SCIATRAN, J. Quant. Spectrosc. Ra., 133, 13–71, doi:10.1016/j.jqsrt.2013.07.004, 2014.

Russell III., J. M. and Drayson, S. R.: The inference of atmospheric ozone using satellite horizon measurements in the $1042\,cm^{-1}$ band, J. Atmos. Sci., 29, 376–390, 1972.

Russell III., J. M., Gordley, L. L., Park, J. H., Drayson, S. R., Hesketh, W. D., Cicerone, R. J., Tuck, A. F., Frederick, J. E., Harries, J. E., and Crutzen, P. J.: The Halogen Occultation Experiment, J. Geophys. Res., 98, 10777–10797, 1993.

Schneising, O., Buchwitz, M., Reuter, M., Heymann, J., Bovensmann, H., and Burrows, J. P.: Long-term analysis of carbon dioxide and methane column-averaged mole fractions retrieved from SCIAMACHY, Atmos. Chem. Phys., 11, 2863–2880, doi:10.5194/acp-11-2863-2011, 2011.

Schneising, O., Heymann, J., Buchwitz, M., Reuter, M., Bovensmann, H., and Burrows, J. P.: Anthropogenic carbon dioxide source areas observed from space: assessment of regional enhancements and trends, Atmos. Chem. Phys., 13, 2445–2454, doi:10.5194/acp-13-2445-2013, 2013.

Sioris, C. E., Boone, C. D., Nassar, R., Sutton, K. J., Gordon, I. E., Walker, K. A., and Bernath, P. F.: Retrieval of carbon dioxide vertical profiles from solar occultation observations and associated error budgets for ACE-FTS and CASS-FTS, Atmos. Meas. Tech., 7, 2243–2262, doi:10.5194/amt-7-2243-2014, 2014.

von Clarmann, T., Glatthor, N., Grabowski, U., Höpfner, M., Kellmann, S., Kiefer, M., Linden, A., Mengistu Tsidu, G., Milz, M., Steck, T., Stiller, G. P., Wang, D. Y., Fischer, H., Funke, B., Gil-López, S., and López-Puertas, M.: Retrieval of temperature and tangent altitude pointing from limb emission spectra recorded from space by the Michelson Interferometer for Passive Atmospheric Sounding (MIPAS), J. Geophys. Res., 108, 4736, doi:10.1029/2003JD003602, 2003.

Wunch, D., Toon, G. C., Blavier, J.-F. L., Washenfelder, R. A., Notholt, J., Connor, B. J., Griffith, D. W. T., Sherlock, V., and Wennberg, P. O.: The total carbon column observing network, Philos. T. R. Soc. A, 369, 2087–2112, doi:10.1098/rsta.2010.0240, 2011.